Identification of a geometrically nonlinear micromorphic continuum via granular micromechanics

Anil Misra (1), Luca Placidi (2), Francesco dell'Isola (3), Emilio Barchiesi (4,5)

- (1) The University of Kansas. Civil, Environmental and Architectural Engineering Department. 1530 W. 15th Street, Lawrence, KS 66045-7609.
- (2) International Telematic University UNINETTUNO. Faculty of Engineering. Corso Vittorio Emanuele II 39 00186, Roma (Italy). Corresponding: luca.placidi@uninettunouniversity.net
- (3) DICEEA and International Research Center on Mathematics and Mechanics of Complex Systems (M&MoCS). Università degli Studi dell'Aquila. Via Giovanni Gronchi 18 Zona industriale di Pile 67100, L'Aquila, Italy.
- (4) Universidad de Lima, Instituto de Investigación Científica, Av. Javier Prado Este 4600, Santiago de Surco 15023, Perù.
- (5) École Nationale d'Ingénieurs de Brest, ENIB, UMR CNRS 6027, IRDL, F-29200 Brest, France.

Abstract

Describing the emerging macro-scale behavior by accounting for the micro-scale phenomena calls for microstructure-informed continuum models accounting properly for the deformation mechanisms identifiable at the micro-scale. Classical continuum theory, in contrast to the micromorphic continuum theory, is unable to take into account the effects of complex kinematics and distribution of elastic energy in internal deformation modes within the continuum material point. In this paper, we derive a geometrically non-linear micromorphic continuum theory on the basis of granular mechanics, utilizing grain-scale deformation as the fundamental building block. The definition of objective kinematic descriptors for relative motion is followed by Piola's ansatz for micro-macro kinematic bridging and, finally, by a limit process leading to the identification of the continuum stiffness parameters in terms of few micro-scale constitutive quantities. A key aspect of the presented approach is the identification of relevant kinematic measures that describe the deformation of the continuum body and link it to the micro-scale deformation. The methodology, therefore, has the ability to reveal the connections between the micro-scale mechanisms that store elastic energy and lead to particular emergent behavior at the macro-scale.

keywords: micromorphic continuum, microstructured solids, granular micromechanics, higher-order theories, finite deformations

1 Introduction

Micromorphic continuum models provide an approach to describe micro-scale structural and mechanical effects in the continuum description of material behavior [1–4]. For micromorphic models to be representative, it is important to link the continuum fields with the micro-scale mechanisms. For instance, when we seek descriptions of the collective behavior of a large number of grains, as in the case in which a material's granular microstructural effect need to be modeled, it is necessary to describe the effects of grain and grain-grain interface deformations (termed as micromechanics), which could be highly localized and directional, as in the case of Hertzian contacts [5,6]. These grain

deformations could be non-uniform due to the grain-shape and interfacial/surfacial characteristics or due to the grain-neighborhood structure (termed as microstructure). The grains can also experience rotations relative to their neighboring grains further contributing to the overall deformation of the collective system [7,8]. These peculiarities of granular systems renders the modeling of the behavior that emerges at the macro-scale (containing large number of grains) particularly challenging. It is now widely accepted that the classical continuum approach (or the Cauchy format) fails woefully in representing the true nature of the micro-structured material behavior and describe many observed phenomena at the macro-scale, even though it serves well for a number of engineering problems. There is growing realization that to describe the emerging macro-scale behavior of these materials faithfully and with increasing fidelity, it is necessary to consider continuum models in which the deformations at micro-scale are properly accounted. A key shortcoming of the classical continuum theory is its inability to describe the effects of complex kinematics and distribution of elastic energy in internal deformation modes within the continuum material point. In this regard, it is worthwhile to recall that in the early development of the continuum modeling of deformable media in the works of Navier, Cauchy, Poisson and Piola, the material was viewed as composed of molecules (particles) that attract and repel each other [9-11]. Many materials, particularly at the scale in which granular microstructures appear, can be treated in a similar sense in which the deformation of an interacting grain-pair can be effectively described in terms of the relative movements of the grain centroids/barycenters regardless of the location of the actual deformation within the grains. Indeed such a treatment can serve as a point of departure for both discrete and continuum models. Examples of discrete models range from atomistic and molecular (see among a very large literature base [12,13]) to more recent large grain models (see among others [14,15]). Continuum models of these materials that proceed from this approach are traced to early part of 20th century (see historical context in the review [16]) to more recent models such as those in [7,17,18] devised for the case of small deformations to account for internal deformation modes.

In discrete models the key kinematic variable is the grain motion, thus by their nature, these models describe the fate of every grain as a result of its interactions with the neighbors and by extension the whole collection. Discrete models, therefore, can result in grain trajectories (that can include grain translations and grain spins) and spatial distributions of deformation energies and their potential decomposition into various deformation modes. The extensive approach is also a principal drawback of discrete model as the detailed data is, in many cases, distinguished by the lack of accurate knowledge of grain locations, shapes and surface type/conditions and every possible grain-pair interaction relationships. Nevertheless, simulations using discrete models [19–29] have been suggestive and have led to the recognition of certain micro-scale phenomena, such as localization of energy into small zones of grain/atomic clusters [30, 31] or localization bands and vortices [32,33], propensity of micro-rotation [34], identification of floppy modes [35], and so-called 'force-chains' (see for example [14, 36–38]). Many of these micro-scale phenomena, particularly those related to certain clustering of grain displacements and coherent/incoherent grain rotations, are attested to by experimental measurements of grain motions such as [39, 40]. For describing the many relevant phenomena exhibited by grain collections detailed information regarding precise grain trajectory is unnecessary. However, the grain-scale kinematics have profound relevance in the macro-scale description of granular materials representing the emergent collective behavior of large number of grains. Indeed, the practical pathway to the control of macro-scale behavior by accessing the micro-scale lies in their representative linkages based upon predictive theories [41]. The recent realization of metamaterials based upon pantographic motif that link to second gradient continuum description [42–50] and chiral granular materials that link to Cosserat continuum are exemplar of such predictive micro-macro theoretical identifications [51-54]. These works have shown that successful efforts to link micro- to macro-scale lead to generalized continuum theories and these can, therefore provide efficient ways for rational design of (meta)materials (as opposed to trial and error or other ad hoc approaches, see for example the review by [55, 56]). Remarkably these micro-macro identifications indicate how the stored elastic energy can be distributed within internal deformation modes, including second [57–69] and higher [35] gradient modes, grain rotations/spins [7], and nonstandard coupling of shear and rotations [70, 71].

In the spirit of developing such micro-macro identifications in a generalized setting of finite deformations that account for geometric nonlinearity, we focus in this paper upon a micromorphic continuum description of materials in which granular microstructural effects need to be modeled. In these cases, Taylor expansion of only conventional macro-scale kinematic descriptor is not representative and additional kinematic descriptors may be introduced to accurately describe the response as in Cosserat or micromorphic media [17, 18, 51, 72-83]. To this end we utilize neighboring grain-pair deformation as the fundamental building block and develop objective kinematic descriptors for relative displacements following Piola's ansatz for micro-macro identification. Micro-scale deformation energy is then introduced in terms of the developed objective relative displacement decomposed into a component along the vector that represents the directors of generic grain-pairs centroids in the system, termed as normal component, and a component in the orthogonal plane, termed as tangential component. For the present work, a quadratic form of the micro-scale deformation energy is utilized to obtain an identification for the case of geometrically non-linear isotropic elasticity. As a result, expressions for elastic constants of a linear novel micromorphic continuum are obtained in terms of the micro-scale parameters. The plan of the paper is the following. Subsequent to this introduction, in Sec. 2, the discrete and continuous models describing a granular system are presented. Particularly, the discrete model, whose kinematics is ultimately specified in terms of a position and a micromorphic deformation gradient for each subsystem - a granular aggregate – termed here as sub-body is introduced first. The continuum model is then introduced and discrete-continuum kinematic bridging is performed through the Piola's ansatz. Specialization of the proposed approach to Cosserat and strain-gradient continua through proper restrictions of the micromorphic deformation gradient is subsequently discussed. Section 3 builds on the previous sections, which are exclusively concerned with the kinematics of the studied systems, by introducing the elastic strain energy for the discrete model and the corresponding one for the continuum model as the result of a homogenization procedure based on the Piola's ansatz. More specifically, relative deformation measures are introduced followed by the definition of the elastic strain energy function in the nonlinear case. Special emphasis is given to the nonlinear 3D isotropic case for no intergranular micromorphic deformation effects and to the linear 3D isotropic case for general intergranular micromorphic deformations. Finally, conclusions are briefly presented.

2 Discrete and continuous models for granular systems

2.1 Discrete model

For a material with granular microstructure, the discrete granular model is illustrated, as a general example, in Fig. 2.1. In the reference configuration we have N sub-bodies. Each sub-body is composed by many grains and is assumed to be a continuum, one point of which is labeled $X_n \in B_n$ with n = 1, ... N. All other points of the sub-body are labeled $X'_n \in B_n$. When this material undergoes deformation, the point X_n is placed, in the present configuration, at x_n via the placement function x_n , i.e.,

$$x_n = \chi_n(t), \quad \forall t \in \mathbb{R}, \quad \forall n = 1, \dots, N,$$
 (1)

where t is the time variable. While all the other points $X'_n \in B_n$ of the grain n are placed, in the present configuration, at x'_n via a different placement function χ'_n , i.e.,

$$x'_n = \chi'_n(X'_n, t), \quad \forall t \in \mathbb{R}, \quad \forall X'_n \in B_n, \quad \forall n = 1, \dots, N,$$
 (2)

in such a way that, evaluating this second placement function at $X'_n = X_n$, we have

$$\chi'_{n}(X_{n},t) = \chi_{n}(t), \quad \forall t \in \mathbb{R}, \quad \forall n = 1,\ldots, N.$$

The sub-body B_n is assumed to be sufficiently small that a Taylor's series expansion of χ'_n centered at $X'_n = X_n$ can be truncated at the first order, i.e.,

$$x'_{n} = \chi'_{n}(X'_{n}, t) = \chi_{n}(t) + P_{n}(t)(X'_{n} - X_{n}), \quad \forall t \in \mathbb{R}, \quad \forall n = 1, \dots, N$$

$$(3)$$

where deformation gradients are defined,

$$P_n(t) = \left. \frac{\partial \chi'_n}{\partial X'_n} \right|_{X'_n = X_n},$$

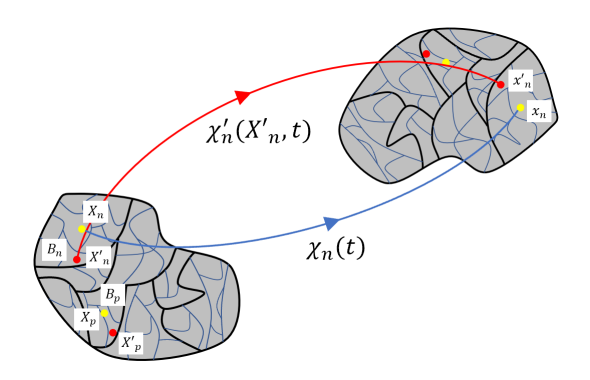


Figure 1: Discrete model. Each sub-body B_n with $n=1,\ldots N$ in the reference configuration is represented with black boundaries and is composed by many grains. Each grain is represented with blue boundaries. For each sub-body B_n , two placements are defined. The placement of the point X_n , belonging to one of the grain of the sub-body B_n , is $\chi_n(t)$, according to (1). The placement of the point X'_n , belonging eventually to another grain of the sub-body B_n , is $\chi'_n(X'_n,t)$, according to (2).

and the truncation is equivalent to assuming an affine deformation of each sub-body B_n .

Thus, the kinematics of the discrete model is completely described, for each sub-body B_n , by the following two functions

$$\chi_n(t), P_n(t), \quad \forall t \in \mathbb{R}, \quad \forall n = 1, \dots, N.$$

2.2 Continuum model

The continuum model is described in Fig. 2. In the reference configuration we have a continuum body C^* . Each point of this continuum is called $X \in C^*$. The same point X is the representative of a micro-structure at a different, smaller scale, and may be another continuum. Any point within this micro-structure is called X'. The point X is placed, in the present configuration, at x via the placement function χ , i.e.,

$$x = \chi(X, t), \quad \forall t \in \mathbb{R}, \quad \forall X \in C^*.$$
 (4)

Further, the points X' of the micro-structure are placed, in the present configuration, at x' via a different placement function χ' , i.e.,

$$x' = \chi'(X, X', t), \quad \forall t \in \mathbb{R}, \quad \forall X \in C^*, \tag{5}$$

in such a way that, evaluating it at X' = X, we have

$$\chi'(X, X, t) = \chi(X, t), \quad \forall t \in \mathbb{R}, \quad \forall X \in C^*.$$
 (6)

The micro-structure is assumed to be sufficiently small that a Taylor's series expansion of the placement function $\chi'(X, X', t)$ centered at X' = X can be truncated at the first order, i.e.,

$$x' = \chi'(X, X', t) = \chi(X, t) + P(X, t)(X' - X), \quad \forall t \in \mathbb{R}, \quad \forall X \in C^*$$

$$(7)$$

where the micromorphic deformation gradient $\mathcal{P} = P(X, t)$ of each micro-structure is defined,

$$\mathcal{P} = P(X, t) = \left. \frac{\partial \chi'}{\partial X'} \right|_{X' = X}, \quad \forall t \in \mathbb{R}, \quad \forall X \in C^*.$$
 (8)

and where (6) has been considered. The truncation of (7) at first order is equivalent to assume an affine deformation of each micro-structure. Thus, the kinematics of the continuum model is completely described by the following couple of functions

$$\chi(X,t), P(X,t), \forall t \in \mathbb{R}, \forall X \in C^*.$$

The deformation gradient, in this case, is defined by two gradients: the gradient $\nabla \chi$ of the placement function, and the gradient ∇P of the micromorphic deformation gradient

$$\mathcal{F} = F(X, t) = \nabla \chi = \frac{\partial \chi}{\partial X}, \qquad \nabla P = \frac{\partial P}{\partial X}.$$
 (9)

Thus, the Green-Saint-Venant tensor G (or non-linear macro-strain) and the micromorphic Green-Saint-Venant tensor M are defined as in (10)

$$G = \frac{1}{2} \left(\mathcal{F}^T \mathcal{F} - I \right), \quad M = \frac{1}{2} \left(\mathcal{P}^T \mathcal{P} - I \right), \tag{10}$$

In addition, a relative micro-macro Green-Saint-Venant tensor (or non-linear relative deformation) is defined as

$$\Upsilon = (I - \mathcal{P}^T \mathcal{F}^{-T}). \tag{11}$$

Note that the tensor Υ defined in (11) vanishes when $\mathcal{P} \equiv \mathcal{F}$, i.e. when the micromorphic deformation gradient \mathcal{P} equals the deformation gradient \mathcal{F} . Such a tensor is nothing but a strain measure taking into account the differential deformations of the continuum element and the microstructure. Further, considering that a polar decomposition holds for both the micromorphic deformation gradient and the macro deformation gradient, it can be concluded that the tensor Υ takes into account also the differential rotation between the micro- and macro-scale. Remark that, as it will be shown in the sequel, the definition of Υ in (11) is only one of the possible non-linear generalizations of the relative deformation γ defined in Mindlin's work [1]. It is also worthwhile to define the following third order tensors, the so-called first and second non-linear micro-deformation gradients

$$\Lambda = \left(\mathcal{F}^{-1}\nabla P\right)^{T_{13}}, \quad \Lambda^r = \left(\mathcal{P}^T\nabla P\right)^{T_{13}} \tag{12}$$

where the transpose operator T_{13} refers to the first and to the third indices of the third order tensors Λ and Λ^r as better defined in index notation as follows,

$$\Lambda_{ijh} = \left(\left[\mathcal{F}^{-1} \nabla P \right]^{T_{13}} \right)_{ijh} = \left(\mathcal{F}^{-1} \nabla P \right)_{hji} = \left(\mathcal{F}^{-1} \right)_{ha} \left(\nabla P \right)_{aji} = \mathcal{F}_{ha}^{-1} P_{aj,i}, \tag{13}$$

$$\Lambda_{ijh}^{r} = \left(\left[\mathcal{P}^{T} \nabla P \right]^{T_{13}} \right)_{ijh} = \left(\mathcal{P}^{T} \nabla P \right)_{hji} = \left(\mathcal{P}^{T} \right)_{ha} (\nabla P)_{aji} = \mathcal{P}_{ah} P_{aj,i}. \tag{14}$$

We remark that the tensors defined in (10), (11) and (12) are objective as shown in the following. Let Q be a general orthogonal matrix giving a change of the frame of reference, let $[\mathcal{F}]$ be the matrix representation of the deformation gradient \mathcal{F} , $[\mathcal{P}]$ be that of the micromorphic deformation gradient \mathcal{P} and $[\nabla P]$ be that of its gradient. This leads to

$$\left[\overline{\mathcal{F}}\right] = Q\left[\mathcal{F}\right], \quad \left[\overline{\mathcal{P}}\right] = Q\left[\mathcal{P}\right], \quad \left[\overline{\nabla P}\right] = Q\left[\nabla P\right],$$

where $[\mathcal{F}]$, $[\mathcal{P}]$ and $[\nabla P]$ are the matrix representations of the same tensors \mathcal{F} , \mathcal{P} and ∇P , respectively, in the rotated, via Q, frame of reference. It is straightforward to show that the matrix representation [G] of the Green-Saint-Venant tensor in this rotated frame of reference is the same as that in the initial frame of reference, denoted by [G],

$$\left[\overline{G}\right] = \frac{1}{2} \left(\left[\overline{\mathcal{F}}\right]^T \left[\overline{\mathcal{F}}\right] - [I] \right) = \frac{1}{2} \left(\left[\mathcal{F}\right]^T Q^T Q \left[\mathcal{F}\right] - [I] \right) = \frac{1}{2} \left(\left[\mathcal{F}\right]^T \left[\mathcal{F}\right] - [I] \right) = \left[G\right],$$

where [I] is the identity matrix. The same frame indifference can be demonstrated for the micromorphic Green-Saint-Venant tensor M, using the matrix representations $[\overline{M}]$ and [M] as

$$\left[\overline{M}\right] = \frac{1}{2} \left(\left[\overline{\mathcal{P}} \right]^T \left[\overline{\mathcal{P}} \right] - [I] \right) = \frac{1}{2} \left(\left[\mathcal{P} \right]^T Q^T Q \left[\mathcal{P} \right] - [I] \right) = \frac{1}{2} \left(\left[\mathcal{P} \right]^T \left[\mathcal{P} \right] - [I] \right) = [M],$$

for the relative micro-macro Green-Saint-Venant tensor Υ , using the matrix representations $\boxed{\Upsilon}$ and $\boxed{\Upsilon}$ as

$$\left[\overline{\Upsilon}\right] = \left[I\right] - \left[\overline{\mathcal{P}}\right]^T \left[\overline{\mathcal{F}}\right]^{-T} = \left[\mathcal{P}\right]^T Q^T Q \left[\mathcal{F}\right]^{-T} - I = \left[\mathcal{P}\right]^T \left[\mathcal{F}\right]^{-T} - I = \left[\Upsilon\right],$$

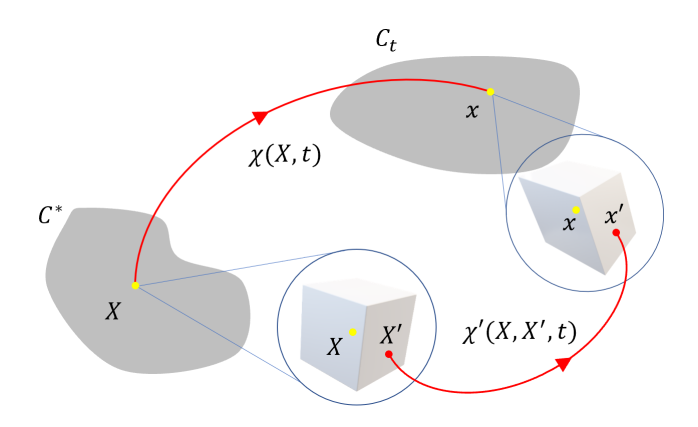


Figure 2: Continuum model. The reference configuration of the continuum body is C^* . Each point of it is called $X \in C^*$ and its placement is $\chi(X,t)$. Such a point X is the representative of a micro-structure, e.g. the cube in the figure. Within the micro-structure (thus, within the cube in the figure) two placements are defined. The first, according to (4), is the same placement $\chi(X,t)$ of the point X. The second, according to (5), placement $\chi'(X,X',t)$ define that of any other points X' of the micro-structure.

for the first relative micro-deformation gradient using with the matrix representations $[\Lambda]$ and $[\Lambda]$ (or with that of its transpose 1-3 counterparts $[\overline{\Lambda}^{T_{13}}]$ and $[\Lambda^{T_{13}}]$) as

$$\left[\overline{\Lambda}^{T_{13}}\right] = \left[\overline{\mathcal{F}}\right]^{-1} \left[\overline{\nabla P}\right] = \left[\mathcal{F}\right]^{-1} Q^T Q \left[\nabla P\right] = \left[\mathcal{F}\right]^{-1} \left[\nabla P\right] = \left[\Lambda^{T_{13}}\right].$$

and, for the second relative micro-deformation gradient, using the matrix representations $[\overline{\Lambda}_r]$ and $[\Lambda_r]$ (or with that of its transpose 1-3 counterparts $[\overline{\Lambda}_r^{T_{13}}]$ and $[\Lambda_r^{T_{13}}]$) as,

$$\left[\overline{\Lambda}_{r}^{T_{13}}\right]=\left[\overline{\mathcal{P}}\right]^{T}\left[\overline{\nabla P}\right]=\left[\mathcal{P}\right]^{T}Q^{T}Q\left[\nabla P\right]=\left[\mathcal{P}\right]^{T}\left[\nabla P\right]=\left[\Lambda_{r}^{T_{13}}\right].$$

2.3 Identification via Piola's ansatz

In the continuum-discrete models identification, we follow Piola's ansatz, such that

$$\chi(X_i, t) = \chi_i(t), \qquad P(X_i, t) = P_i(t), \qquad \forall i = 1, ..., N, \quad \forall t \in \mathbb{R}.$$
 (15)

The (15) implies that the placements $\chi_i(t)$ and the micro-deformation $P_i(t)$, with i=1,...,N, of the N sub-bodies B_n in the discrete model illustrated in Fig. 2.1 correspond to the placement $\chi(X,t)$ and the micro-deformation P(X,t), evaluated respectively at the points X_i with i=1,...,N, of the body C^* in the continuous model given in Fig. 2. With this in mind, we will utilize the discrete model only as a guiding justification for the constitutive assumptions postulated in the following Section 3. Needless to say, the content of this paper refers to the continuous model of Fig. 2. The connection with the discrete model is only suggestive of possible micro-scale mechanism that could be revealed through the Piola's ansatz (15) and is useful for the introduction of the indicated constitutive assumptions. We note that no attempt is made here to give an evolution equation of each grain as one would for a completely discrete description.

2.4 Cosserat and strain-gradient continua obtained by proper restrictions of the micro-deformation \mathcal{P}

We note that restrictions on the micro-deformation $\mathcal{P} = P(X, t)$ define different type of microstructural continua. First of all, no restriction on \mathcal{P} defines a micromorphic continua, but (i) an orthogonal micro-deformation \mathcal{P} define from (10) Cosserat continua,

$$\mathcal{P} \in Orth, \implies M = 0,$$

and (ii) second gradient continua are obtained when the micro-deformation \mathcal{P} is identified with the deformation gradient \mathcal{F} ,

$$\mathcal{P} = \mathcal{F} = (\nabla \chi)$$
,

that implies (iia) zero non-linear relative deformation Υ from (11), (iib) identification of the Green-Saint-Venant tensor G and of the micromorphic Green-Saint-Venant tensor M from (10),

$$\Upsilon = 0, \qquad G = M,$$

(iic) identification of the 13-transpose second relative micro-deformation gradient Λ^r and non-linear macro-strain-gradient tensor ∇G ,

$$(\Lambda^r)^{T_{13}} = \mathcal{P}^T \nabla P = \mathcal{F}^T \nabla F = \nabla G,$$

and (iid) the following relation between the first relative micro-deformation gradient Λ and the non-linear macro-strain-gradient ∇G ,

$$(\Lambda)^{T_{13}} = \mathcal{P}^T \nabla P = \mathcal{F}^{-1} \nabla F = \mathcal{F}^{-1} \mathcal{F}^{-T} \mathcal{F}^T \nabla F = C^{-1} \nabla G,$$

where the left Cauchy-Green deformation tensor C is defined,

$$C = \mathcal{F}^T \mathcal{F}.$$

3 Elastic strain energy

3.1 Relative deformation measures

Let us now assume that two sub-bodies, n and p, respectively placed in the reference configuration at X_n and X_p , are neighboring ones, that their distance is L in the reference configuration and that the unit vector \hat{c} is defined as follows,

$$X_n - X_p = \hat{c}L. \tag{16}$$

In the reference configuration, therefore, the vector attached to the position X_n and pointing to the position X_p is $\hat{c}L$ and given in (16). Further, let us restrict the present model to the case in which the sub-bodies, n and p, place and deform similarly in the present configuration, and therefore the following Taylor's series expansions are possible and yield

$$\chi(X_n, t) \cong \chi(X_p, t) + (\nabla \chi)_{X_n} (X_n - X_p) = \chi(X_p, t) + \mathcal{F}(X_n - X_p).$$
(17)

$$P(X_n, t) \cong P(X_p, t) + (\nabla P)_{X_p}(X_n - X_p).$$
(18)

$$F\left(X_{n},t\right) \cong F\left(X_{n},t\right). \tag{19}$$

We can now define the following 3 objective tensors that may be utilized to represent the material deformation that are traceable to the micro-scale grain-pair relative displacements

$$g^{np}(t) = \frac{1}{2} \left[F^T(X_p, t) F(X_n, t) - I \right], \qquad (20)$$

$$m^{np}(t) = \frac{1}{2} \left[P^T(X_p, t) P(X_n, t) - I \right],$$
 (21)

$$\gamma^{np}(t) = I - P^{T}(X_{n}, t) F^{-T}(X_{p}, t), \qquad (22)$$

where the superscripts n and p refers to the microstructures placed at X_n and at X_p . We call the tensor g^{np} in (20) the macro deformation, the tensor m^{np} in (21) the micro deformation and the tensor γ^{np} in (22) the micro-macro deformation. The proof of their objectivity is analogous with that derived at the end of subsection 2.2.

By insertion of the Taylor's series expansions (18-19) into the 3 definitions (20-21-22), yield, respectively,

$$g^{np}(t) = \frac{1}{2} \left[F^T(X_p, t) F(X_n, t) - I \right] = \frac{1}{2} \left[F^T(X_p, t) F(X_p, t) - I \right], \tag{23}$$

$$m^{np}(t) = \frac{1}{2} \left[P^{T}(X_{p}, t) P(X_{n}, t) - I \right] =$$

$$= \frac{1}{2} \left[P^{T}(X_{p}, t) P(X_{p}, t) - I \right] + \frac{1}{2} P^{T}(X_{p}, t) (\nabla P)_{X_{p}} (X_{n} - X_{p}),$$
(24)

$$\gamma^{np}(t) = I - P^{T}(X_{n}, t) F^{-T}(X_{p}, t) =$$

$$= I - P^{T}(X_{p}, t) F^{-T}(X_{p}, t) - \left[\left(\nabla P^{T} \right)_{X_{p}} (X_{n} - X_{p}) \right] F^{-T}(X_{p}, t) . \tag{25}$$

The use of objective Green-Saint-Venant tensors in (10), (11) and (12) into (23), (24) and (25), yield,

$$g^{np} = G (26)$$

$$m^{np} = M + \frac{L}{2} P^T \nabla P \hat{c} = M + \frac{L}{2} \left(\hat{c} \Lambda^r \right)^T$$
(27)

$$\gamma^{np} = \Upsilon - L\left[\left(\nabla P^{T}\right)\hat{c}\right]F^{-T} = \Upsilon - L\hat{c}\Lambda \tag{28}$$

The last two equations are derived easily in index notation as follows

$$m_{ij}^{np} = M_{ij} + \frac{L}{2} \left(P^T \right)_{ia} (\nabla P)_{ajk} \, \hat{c}_k = M_{ij} + \frac{L}{2} P_{ai} P_{aj,k} \hat{c}_k = M_{ij} + \frac{L}{2} \Lambda_{kji}^r \hat{c}_k,$$

$$\gamma_{ij}^{np} = \Upsilon_{ij} - L \left(\nabla P^T \right)_{iab} \hat{c}_b \left(F^{-T} \right)_{aj} = \Upsilon_{ij} - L P_{ai,b} \hat{c}_b F_{ja}^{-1} = \Upsilon_{ij} - L F_{ja}^{-1} P_{ai,b} \hat{c}_b = \Upsilon_{ij} - L \hat{c}_b \Lambda_{bij},$$

where the definitions (13) and (14) have been considered.

Thus, we define the objective relative displacement, i.e. the macro-relative displacement, with (26),

$$u^{np} = 2Lg^{np}\hat{c} = 2LG\hat{c},\tag{29}$$

the micro-macro-relative displacement, with (28),

$$d^{np} = L\gamma^{np}\hat{c} = L\left(\Upsilon - L\hat{c}\Lambda\right)\hat{c} \tag{30}$$

and the micro-relative displacement, with (27),

$$r^{np} = 2Lm^{np}\hat{c} = 2LM\hat{c} + L^2\hat{c}\left(\hat{c}\Lambda^r\right) \tag{31}$$

that, in index notation, are

$$u_i^{np} = 2LG_{ij}\hat{c}_j, \qquad d_i^{np} = L\Upsilon_{ij}\hat{c}_j - L^2\Lambda_{bij}\hat{c}_b\hat{c}_j, \qquad r_i^{np} = 2LM_{ij}\hat{c}_j + L^2\Lambda_{abi}^r\hat{c}_a\hat{c}_b$$

The half projection of the objective relative displacements on the unit vector \hat{c} , defined in (16), is the so called normal displacements u_{η} . In the same way d_{η} is defined as the normal micro-relative displacement and r_{η} is defined as the normal micro-relative displacement,

$$u_{\eta} = \frac{1}{2} u^{np} \cdot \hat{c} = LG_{ij} \hat{c}_i \hat{c}_j, \quad d_{\eta} = d^{np} \cdot \hat{c} = L\Upsilon_{ij} \hat{c}_j \hat{c}_i - L^2 \Lambda_{abc} \hat{c}_a \hat{c}_b \hat{c}_c, \tag{32}$$

$$r_{\eta} = r^{np} \cdot \hat{c} = 2LM_{ij}\hat{c}_j\hat{c}_i + L^2\Lambda^r_{abc}\hat{c}_a\hat{c}_b\hat{c}_c. \tag{33}$$

Their squares are

$$u_{\eta}^{2} = (LG_{ij}\hat{c}_{i}\hat{c}_{j}) (LG_{ab}\hat{c}_{a}\hat{c}_{b}),$$

$$d_{\eta}^{2} = (L\Upsilon_{ij}\hat{c}_{j}\hat{c}_{i} - L^{2}\Lambda_{ijh}\hat{c}_{i}\hat{c}_{j}\hat{c}_{h}) (L\Upsilon_{ab}\hat{c}_{a}\hat{c}_{b} - L^{2}\Lambda_{abc}\hat{c}_{a}\hat{c}_{b}\hat{c}_{c}),$$

$$r_{\eta}^{2} = (2LM_{ij}\hat{c}_{j}\hat{c}_{i} + L^{2}\Lambda_{ijh}^{r}\hat{c}_{i}\hat{c}_{j}\hat{c}_{h}) (2LM_{ab}\hat{c}_{a}\hat{c}_{b} + L^{2}\Lambda_{abc}^{r}\hat{c}_{a}\hat{c}_{b}\hat{c}_{c}),$$

and therefore

$$u_n^2 = L^2 G_{ij} G_{ab} \hat{c}_i \hat{c}_j \hat{c}_a \hat{c}_b, \tag{34}$$

$$d_{\eta}^2 = L^2 \Upsilon_{ij} \Upsilon_{ab} \hat{c}_i \hat{c}_j \hat{c}_a \hat{c}_b - 2L^3 \Upsilon_{ij} \Lambda_{abc} \hat{c}_i \hat{c}_j \hat{c}_a \hat{c}_b \hat{c}_c + L^4 \Lambda_{ijh} \Lambda_{abc} \hat{c}_i \hat{c}_j \hat{c}_h \hat{c}_a \hat{c}_b \hat{c}_c, \tag{35}$$

$$r_{\eta}^{2} = 4L^{2}M_{ij}M_{ab}\hat{c}_{i}\hat{c}_{j}\hat{c}_{a}\hat{c}_{b} + 4L^{3}M_{ij}\Lambda_{abc}^{r}\hat{c}_{i}\hat{c}_{j}\hat{c}_{a}\hat{c}_{b}\hat{c}_{c} + L^{4}\Lambda_{ijh}^{r}\Lambda_{abc}^{r}\hat{c}_{i}\hat{c}_{j}\hat{c}_{h}\hat{c}_{a}\hat{c}_{b}\hat{c}_{c},$$
(36)

$$u_{\eta}d_{\eta} = L^2 G_{ij} \Upsilon_{ab} \hat{c}_i \hat{c}_j \hat{c}_a \hat{c}_b - L^3 G_{ij} \Lambda_{abc} \hat{c}_i \hat{c}_j \hat{c}_h \hat{c}_a \hat{c}_b \hat{c}_c, \tag{37}$$

$$u_n r_n = 2L^2 G_{ij} M_{ab} \hat{c}_i \hat{c}_j \hat{c}_a \hat{c}_b + L^3 G_{ij} \Lambda^r_{abc} \hat{c}_i \hat{c}_j \hat{c}_b \hat{c}_a \hat{c}_b \hat{c}_c, \tag{38}$$

$$r_{\eta}d_{\eta} = 2L^{2}M_{ij}\Upsilon_{ab}\hat{c}_{i}\hat{c}_{j}\hat{c}_{a}\hat{c}_{b} + L^{3}\Upsilon_{ij}\Lambda_{abc}^{r}\hat{c}_{i}\hat{c}_{j}\hat{c}_{h}\hat{c}_{a}\hat{c}_{b}\hat{c}_{c} -L^{3}M_{ij}\Lambda_{abc}\hat{c}_{i}\hat{c}_{i}\hat{c}_{h}\hat{c}_{a}\hat{c}_{b}\hat{c}_{c} - L^{4}\Lambda_{ijh}^{r}\Lambda_{abc}\hat{c}_{i}\hat{c}_{j}\hat{c}_{h}\hat{c}_{a}\hat{c}_{b}\hat{c}_{c}.$$

$$(39)$$

The tangent displacement u_{τ} is defined

$$u_{\tau} = u^{np} - (u^{np} \cdot \hat{c}) \,\hat{c}. \tag{40}$$

as well as its square

$$u_{\tau}^{2} = u^{np} \cdot u^{np} - u_{n}^{2} = 4L^{2}G_{ij}G_{ab}\left(\delta_{ia}\hat{c}_{j}\hat{c}_{b} - \hat{c}_{i}\hat{c}_{j}\hat{c}_{a}\hat{c}_{b}\right) \tag{41}$$

The tangent micro-macro-relative displacement d_{τ} and the tangent micro-relative displacement r_{τ} are defined

$$d_{\tau} = d^{np} - (d^{np} \cdot \hat{c}) \,\hat{c}. \tag{42}$$

$$r_{\tau} = r^{np} - (r^{np} \cdot \hat{c}) \,\hat{c}. \tag{43}$$

Thus, their squares are calculated as follows

$$d_{\tau}^{2} = L^{2} \Upsilon_{ij} \Upsilon_{ab} \left[\hat{c}_{j} \hat{c}_{b} \delta_{ia} - \hat{c}_{i} \hat{c}_{j} \hat{c}_{a} \hat{c}_{b} \right] \tag{44}$$

$$-2L^{3}\Upsilon_{ij}\Lambda_{abc}\left[\hat{c}_{j}\hat{c}_{a}\hat{c}_{c}\delta_{ib}-\hat{c}_{i}\hat{c}_{j}\hat{c}_{a}\hat{c}_{b}\hat{c}_{c}\right]+L^{4}\Lambda_{ijh}\Lambda_{abc}\left[\hat{c}_{i}\delta_{jb}\hat{c}_{h}\hat{c}_{a}\hat{c}_{c}-\hat{c}_{i}\hat{c}_{j}\hat{c}_{h}\hat{c}_{a}\hat{c}_{b}\hat{c}_{c}\right],$$

$$r_{\tau}^2 = 4L^2 M_{ij} M_{ab} \left[\hat{c}_j \hat{c}_b \delta_{ia} - \hat{c}_i \hat{c}_j \hat{c}_a \hat{c}_b \right] \tag{45}$$

$$+4L^3M_{ij}\Lambda^r_{abc}\left[\hat{c}_j\hat{c}_a\hat{c}_c\delta_{ib}-\hat{c}_i\hat{c}_j\hat{c}_a\hat{c}_b\hat{c}_c\right]+L^4\Lambda^r_{ijh}\Lambda^r_{abc}\left[\hat{c}_i\delta_{jb}\hat{c}_h\hat{c}_a\hat{c}_c-\hat{c}_i\hat{c}_j\hat{c}_h\hat{c}_a\hat{c}_b\hat{c}_c\right].$$

3.2 Definition of the elastic strain energy function in the nonlinear case

The elastic energy function for a given couple of sub-bodies, say the couple n-p considered in Section 3.1, is assumed to be a quadratic form of normal and tangent components of the macro-relative displacement (29), of the micro-macro-relative displacement (30) and of the micro-relative displacement (31),

$$U^{np} = \frac{1}{2}k_{\eta}u_{\eta}^{2} + \frac{1}{2}k_{\tau}u_{\tau}^{2} + \frac{1}{2}k_{d\eta}d_{\eta}^{2} + \frac{1}{2}k_{d\tau}d_{\tau}^{2} + \frac{1}{2}k_{r\eta}r_{\eta}^{2} + \frac{1}{2}k_{r\tau}r_{\tau}^{2} + k_{ud}u_{\eta}d_{\eta} + k_{ur}u_{\eta}r_{\eta} + k_{rd}r_{\eta}d_{\eta},$$
 (46)

where k_{η} , k_{τ} , $k_{d\eta}$, $k_{d\tau}$, $k_{r\eta}$, $k_{r\tau}$, k_{ud} , k_{ur} and k_{rd} are 9 elastic constitutive coefficients of the present formulation. In principle, in the anisotropic case they all are a function of the unit vector \hat{c} , i.e. they are 9 orientation distribution function of the stiffness of the continuum. In particular, k_{η} and k_{τ} are the normal and tangent stiffness defined and used in [84]. Here the kinematic characterization of the material is more complicated and we have also the normal $k_{d\eta}$ and tangent $k_{d\tau}$ micro-macro-relative stiffness and the normal $k_{r\eta}$ and tangent $k_{r\tau}$ micro-relative stiffness. Besides, the presence of three scalar invariants u_{η} , d_{η} and r_{η} makes possible three kinds of elastic interactions, i.e. the displacement-micro-macro-relative interaction with the homonymous stiffness k_{ut} , the displacement-micro-relative interaction with the homonymous stiffness k_{ut} and the micro-macro-micro-relative interaction with the homonymous stiffness k_{ut} and the micro-macro-micro-relative interaction with the homonymous stiffness k_{ut} and the micro-macro-micro-relative interaction with the homonymous stiffness k_{ut} and the micro-macro-micro-relative interaction with the homonymous stiffness k_{ut} and the micro-macro-micro-relative interaction with the homonymous stiffness k_{ut} and the micro-macro-micro-relative interaction with the homonymous stiffness k_{ut} and the micro-macro-micro-relative interaction with the homonymous stiffness k_{ut} and the micro-macro-micro-relative interaction with the homonymous stiffness k_{ut} and the micro-macro-micro-relative interaction with the homonymous stiffness k_{ut} and the micro-macro-micro-relative interaction with the homonymous stiffness k_{ut} and the micro-macro-micro-relative interaction with the homonymous stiffness k_{ut} and the micro-macro-micro-micro-relative interaction with the homonymous stiffness k_{ut} and the micro-macro-micro-micro

$$\begin{split} U &= \int_{\mathcal{S}^{1,2}} U^{np} = \int_{\mathcal{S}^{1}} \frac{1}{2} k_{\eta} \left(L^{2} G_{ij} G_{ab} \hat{c}_{i} \hat{c}_{j} \hat{c}_{a} \hat{c}_{b} \right) + \frac{1}{2} k_{\tau} \left(4L^{2} G_{ij} G_{ab} \left(\delta_{ia} \hat{c}_{j} \hat{c}_{b} - \hat{c}_{i} \hat{c}_{j} \hat{c}_{a} \hat{c}_{b} \right) \right) \\ &+ \int_{\mathcal{S}^{1,2}} \frac{1}{2} k_{d\eta} L^{2} \Upsilon_{ij} \Upsilon_{ab} \hat{c}_{i} \hat{c}_{j} \hat{c}_{a} \hat{c}_{b} + \frac{1}{2} k_{d\tau} L^{2} \Upsilon_{ij} \Upsilon_{ab} \left[\hat{c}_{j} \hat{c}_{b} \delta_{ia} - \hat{c}_{i} \hat{c}_{j} \hat{c}_{a} \hat{c}_{b} \right] \\ &- \int_{\mathcal{S}^{1,2}} \frac{1}{2} k_{d\eta} 2L^{3} \Upsilon_{ij} \Lambda_{abc} \hat{c}_{i} \hat{c}_{j} \hat{c}_{a} \hat{c}_{b} \hat{c}_{c} + \frac{1}{2} k_{d\tau} 2L^{3} \Upsilon_{ij} \Lambda_{abc} \left[\hat{c}_{j} \hat{c}_{a} \hat{c}_{c} \delta_{ib} - \hat{c}_{i} \hat{c}_{j} \hat{c}_{a} \hat{c}_{b} \hat{c}_{c} \right] \\ &+ \int_{\mathcal{S}^{1,2}} \frac{1}{2} k_{d\eta} L^{4} \Lambda_{ijh} \Lambda_{abc} \hat{c}_{i} \hat{c}_{j} \hat{c}_{h} \hat{c}_{a} \hat{c}_{b} \hat{c}_{c} + \frac{1}{2} k_{d\tau} L^{4} \Lambda_{ijh} \Lambda_{abc} \left[\hat{c}_{i} \delta_{jb} \hat{c}_{h} \hat{c}_{a} \hat{c}_{c} - \hat{c}_{i} \hat{c}_{j} \hat{c}_{h} \hat{c}_{a} \hat{c}_{b} \hat{c}_{c} \right] \\ &+ \int_{\mathcal{S}^{1,2}} \frac{1}{2} k_{d\eta} L^{2} \Lambda_{ijh} \Lambda_{abc} \hat{c}_{i} \hat{c}_{j} \hat{c}_{h} \hat{c}_{a} \hat{c}_{b} \hat{c}_{c} + \frac{1}{2} k_{d\tau} L^{2} \Lambda_{ijh} \Lambda_{abc} \left[\hat{c}_{i} \delta_{jb} \hat{c}_{h} \hat{c}_{a} \hat{c}_{c} - \hat{c}_{i} \hat{c}_{j} \hat{c}_{h} \hat{c}_{a} \hat{c}_{b} \hat{c}_{c} \right] \\ &+ \int_{\mathcal{S}^{1,2}} \frac{1}{2} k_{r\eta} 4L^{2} M_{ij} M_{ab} \hat{c}_{i} \hat{c}_{j} \hat{c}_{a} \hat{c}_{b} \hat{c}_{c} + \frac{1}{2} k_{r\tau} 4L^{2} M_{ij} M_{ab} \left[\hat{c}_{j} \hat{c}_{b} \delta_{ia} - \hat{c}_{i} \hat{c}_{j} \hat{c}_{a} \hat{c}_{b} \hat{c}_{c} \right] \\ &+ \int_{\mathcal{S}^{1,2}} \frac{1}{2} k_{r\eta} 4L^{3} M_{ij} \Lambda_{abc}^{r} \hat{c}_{i} \hat{c}_{j} \hat{c}_{a} \hat{c}_{b} \hat{c}_{c} + \frac{1}{2} k_{r\tau} 4L^{3} M_{ij} \Lambda_{abc}^{r} \left[\hat{c}_{j} \hat{c}_{a} \hat{c}_{b} \hat{c}_{a} - \hat{c}_{i} \hat{c}_{j} \hat{c}_{a} \hat{c}_{b} \hat{c}_{c} \right] \\ &+ \int_{\mathcal{S}^{1,2}} \frac{1}{2} k_{r\eta} L^{4} \Lambda_{ijh}^{r} \Lambda_{abc}^{r} \hat{c}_{i} \hat{c}_{j} \hat{c}_{a} \hat{c}_{b} \hat{c}_{c} + \frac{1}{2} k_{r\tau} L^{4} \Lambda_{ijh}^{r} \Lambda_{abc}^{r} \left[\hat{c}_{i} \delta_{jb} \hat{c}_{h} \hat{c}_{a} \hat{c}_{b} \hat{c}_{c} \right] \\ &+ \int_{\mathcal{S}^{1,2}} k_{r\eta} L^{4} \Lambda_{ijh}^{r} \Lambda_{abc} \hat{c}_{i} \hat{c}_{j} \hat{c}_{h} \hat{c}_{a} \hat{c}_{b} \hat{c}_{c} \\ &+ \int_{\mathcal{S}^{1,2}} k_{r\eta} L^{4} \Lambda_{ijh}^{r} \Lambda_{abc} \hat{c}_{i} \hat{c}_{j} \hat{c}_{h} \hat{c}_{a} \hat{c}_{b} \hat{$$

or, in a compact form we have

$$U = \frac{1}{2} \mathbb{C}_{ijkl} G_{ij} G_{kl} + \frac{1}{2} \mathbb{B}_{ijab} \Upsilon_{ij} \Upsilon_{ab} + \frac{1}{2} \mathbb{A}_{ijhabc} \Lambda_{ijh} \Lambda_{abc}$$

$$+ \mathbb{D}_{ijklm} \Upsilon_{ij} \Lambda_{klm} + \mathbb{F}_{ijklm} \Lambda_{ijk} G_{lm} + \mathbb{G}_{ijkl} \Upsilon_{ij} G_{kl},$$

$$+ \frac{1}{2} \mathbb{C}_{ijkl}^r M_{ij} M_{kl} + \mathbb{D}_{ijklm}^r M_{ij} \Lambda_{klm}^r + \mathbb{D}_{ijklm}^{rr} (\Upsilon_{ij} \Lambda_{klm}^r - M_{ij} \Lambda_{klm})$$

$$+ \frac{1}{2} \mathbb{A}_{ijhabc}^r \Lambda_{ijh}^r \Lambda_{abc}^r + \mathbb{G}_{ijkl}^r M_{ij} G_{kl} + \mathbb{F}_{ijklm}^r \Lambda_{ijk}^r G_{lm} + \mathbb{B}_{ijab}^r M_{ij} \Upsilon_{ab}$$

$$(47)$$

where the elastic stiffness \mathbb{C} , \mathbb{B} , \mathbb{A} , \mathbb{D} , \mathbb{D}^r , \mathbb{D}^r , \mathbb{F} , \mathbb{F}^r , \mathbb{G} , \mathbb{C}^r , \mathbb{A}^r and \mathbb{B}^r are identified in (47) as follows, with the symmetrization induced by the symmetry of the strain tensors G and M

$$\mathbb{C}_{ijkl} = L^2 \int_{\mathcal{S}^{1,2}} (k_{\eta} - 4k_{\tau}) \,\hat{c}_i \hat{c}_j \hat{c}_k \hat{c}_l \tag{48}$$

$$+L^2 \int_{\mathcal{S}^{1,2}} k_\tau \left(\delta_{ik} \hat{c}_j \hat{c}_l + \delta_{il} \hat{c}_j \hat{c}_k + \delta_{jk} \hat{c}_i \hat{c}_l + \delta_{jl} \hat{c}_i \hat{c}_k \right),$$

$$\mathbb{B}_{ijab} = L^2 \int_{\mathcal{S}^{1,2}} \left[(k_{d\eta} - k_{d\tau}) \, \hat{c}_i \hat{c}_a + k_{d\tau} \delta_{ia} \right] \hat{c}_j \hat{c}_b, \tag{49}$$

$$A_{ijhabc} = L^4 \int_{S^{1,2}} \left[(k_{d\eta} - k_{d\tau}) \, \hat{c}_j \hat{c}_b + k_{d\tau} \delta_{jb} \right] \hat{c}_i \hat{c}_h \hat{c}_a \hat{c}_c, \tag{50}$$

$$\mathbb{D}_{ijabc} = -L^3 \int_{S^{1,2}} \left[(k_{d\eta} - k_{d\tau}) \, \hat{c}_i \hat{c}_b + k_{d\tau} \delta_{ib} \right] \hat{c}_j \hat{c}_a \hat{c}_c, \tag{51}$$

$$\mathbb{D}_{ijabc}^{r} = 2L^{3} \int_{S^{1,2}} (k_{r\eta} - k_{r\tau}) \,\hat{c}_{i} \hat{c}_{j} \hat{c}_{b} + \frac{1}{2} k_{r\tau} \left[(\hat{c}_{j} \delta_{ib} + \hat{c}_{i} \delta_{jb}) \right] \hat{c}_{a} \hat{c}_{c}, \tag{52}$$

$$\mathbb{D}_{ijabc}^{rr} = L^3 \int_{S^{1,2}} k_{rd} \hat{c}_i \hat{c}_j \hat{c}_a \hat{c}_b \hat{c}_c, \tag{53}$$

$$\mathbb{F}_{ijklm} = -L^3 \int_{\mathcal{S}^{1,2}} k_{ud} \hat{c}_i \hat{c}_j \hat{c}_k \hat{c}_l \hat{c}_m, \quad \mathbb{F}^r_{ijklm} = L^3 \int_{\mathcal{S}^{1,2}} k_{ur} \hat{c}_i \hat{c}_j \hat{c}_k \hat{c}_l \hat{c}_m, \tag{54}$$

$$\mathbb{G}_{ijkl} = L^2 \int_{\mathcal{S}^{1,2}} k_{ud} \hat{c}_i \hat{c}_j \hat{c}_k \hat{c}_l, \quad \mathbb{G}^r_{ijkl} = L^2 \int_{\mathcal{S}^{1,2}} k_{ur} \hat{c}_i \hat{c}_j \hat{c}_k \hat{c}_l, \tag{55}$$

$$\mathbb{C}_{ijkl}^{r} = 4L^{2} \int_{\mathcal{S}^{1,2}} (k_{r\eta} - k_{r\tau}) \,\hat{c}_{i} \hat{c}_{j} \hat{c}_{k} \hat{c}_{l} + \tag{56}$$

$$+L^2 \int_{\mathcal{S}^{1,2}} k_{r\tau} \left(\delta_{ik} \hat{c}_j \hat{c}_l + \delta_{il} \hat{c}_j \hat{c}_k + \delta_{jk} \hat{c}_i \hat{c}_l + \delta_{jl} \hat{c}_i \hat{c}_k \right),$$

$$\mathbb{A}_{ijhabc}^{r} = \frac{1}{2} L^{4} \int_{\mathbb{S}^{1,2}} (k_{r\eta} - k_{r\tau} - 2k_{rd}) \, \hat{c}_{i} \hat{c}_{j} \hat{c}_{h} \hat{c}_{a} \hat{c}_{b} \hat{c}_{c} + k_{r\tau} \hat{c}_{i} \delta_{jb} \hat{c}_{h} \hat{c}_{a} \hat{c}_{c}, \tag{57}$$

$$\mathbb{B}_{ijab}^r = 2L^2 \int_{\mathcal{S}^{1,2}} k_{rd} \hat{c}_i \hat{c}_j \hat{c}_k \hat{c}_l. \tag{58}$$

3.3 Nonlinear 3D isotropic case in absence of micro deformation m^{np}

Let us assume that the micro deformation m^{np} do not have a role in contributing to the elastic deformation energy (47). In this case, we can see from (31) that the micro-relative displacement r^{np} does not contribute to the elastic deformation energy (47). The consequence is that micro-relative displacement r_{η} and r_{τ} play no role in the elastic energy expression (47), as seen from (33) and (43). Therefore, we assume that the corresponding stiffness constants with subscript r, are null, that is

$$k_{r\eta} = k_{r\tau} = k_{ur} = k_{rd} = 0,$$

Thus from (52), (53), $(54)_2$, $(55)_2$, (56), (57) and (58) we have that the corresponding stiffness tensors with superscripts r,

$$\mathbb{D}^r = 0$$
, $\mathbb{D}^{rr} = 0$, $\mathbb{F}^r = 0$, $\mathbb{G}^r = 0$, $\mathbb{C}^r = 0$, $\mathbb{A}^r = 0$, $\mathbb{B}^r = 0$,

are null and therefore the elastic energy (47) is reduced to be in a form that is the analogous of that in eq. (5.1) in Mindlin [1],

$$U = \frac{1}{2} \mathbb{C}_{ijkl} G_{ij} G_{kl} + \frac{1}{2} \mathbb{B}_{ijab} \Upsilon_{ij} \Upsilon_{ab} + \frac{1}{2} \mathbb{A}_{ijhabc} \Lambda_{ijh} \Lambda_{abc}$$

$$+ \mathbb{D}_{ijklm} \Upsilon_{ij} \Lambda_{klm} + \mathbb{F}_{ijklm} \Lambda_{ijk} G_{lm} + \mathbb{G}_{ijkl} \Upsilon_{ij} G_{kl}.$$

$$(59)$$

We will prove in Subsection 3.4 that (59) is nothing else than a possible non-linear geometric generalization of eq. (5.1) in Mindlin [1]. Besides, in the isotropic case Mindlin [1] in eq. (5.4) has given, among the isotropic identification $\mathbb{D} = 0$ and $\mathbb{F} = 0$ (at the end of page 15 in Mindlin [1]), the following representations

$$\mathbb{C}_{ijkl} = \lambda \delta_{ij} \delta_{kl} + \mu_1 \delta_{ik} \delta_{il} + \mu_2 \delta_{il} \delta_{jk}, \tag{60}$$

$$\mathbb{B}_{ijkl} = b_1 \delta_{ij} \delta_{kl} + b_2 \delta_{ik} \delta_{il} + b_3 \delta_{il} \delta_{ik}, \tag{61}$$

$$\mathbb{G}_{ijkl} = g_1 \delta_{ij} \delta_{kl} + g_2 \delta_{ik} \delta_{il} + g_3 \delta_{il} \delta_{jk}, \tag{62}$$

$$\mathbb{A}_{ijklmn} = a_1 \delta_{ij} \delta_{kl} \delta_{mn} + a_2 \delta_{ij} \delta_{km} \delta_{nl} + a_3 \delta_{ij} \delta_{kn} \delta_{lm}
+ a_4 \delta_{jk} \delta_{il} \delta_{mn} + a_5 \delta_{jk} \delta_{im} \delta_{nl} + a_6 \delta_{jk} \delta_{in} \delta_{lm}
+ a_7 \delta_{ki} \delta_{jl} \delta_{mn} + a_8 \delta_{ki} \delta_{jm} \delta_{nl} + a_9 \delta_{ki} \delta_{jn} \delta_{lm}
+ a_{10} \delta_{il} \delta_{jm} \delta_{kn} + a_{11} \delta_{jl} \delta_{km} \delta_{in} + a_{12} \delta_{kl} \delta_{im} \delta_{jn}
+ a_{13} \delta_{il} \delta_{jn} \delta_{km} + a_{14} \delta_{jl} \delta_{kn} \delta_{im} + a_{15} \delta_{kl} \delta_{in} \delta_{jm},$$
(63)

with those conditions that are made explicit at the end of page 16 in Mindlin [1], i.e.,

$$\mu_1 = \mu_2 = \mu$$
, $g_2 = g_3$, $a_1 = a_6$, $a_2 = a_9$, $a_5 = a_7$, $a_{11} = a_{12}$. (64)

Insertion of (64) into (60), (61), (62) and (63) into the compact form of the strain energy (59) we have

$$\begin{split} U &= \frac{1}{2} \lambda \delta_{ij} \delta_{kl} G_{ij} G_{kl} + \frac{1}{2} \mu \delta_{ik} \delta_{jl} G_{ij} G_{kl} + \frac{1}{2} \mu \delta_{il} \delta_{jk} G_{ij} G_{kl} \\ &+ \frac{1}{2} b_1 \delta_{ij} \delta_{kl} \Upsilon_{ij} \Upsilon_{kl} + \frac{1}{2} b_2 \delta_{ik} \delta_{jl} \Upsilon_{ij} \Upsilon_{kl} + \frac{1}{2} b_3 \delta_{il} \delta_{jk} \Upsilon_{ij} \Upsilon_{kl} \end{split}$$

$$\begin{split} &+\frac{1}{2}a_{1}\delta_{ij}\delta_{kl}\delta_{mn}\Lambda_{ijk}\Lambda_{lmn} + \frac{1}{2}a_{2}\delta_{ij}\delta_{km}\delta_{nl}\Lambda_{ijk}\Lambda_{lmn} + \frac{1}{2}a_{3}\delta_{ij}\delta_{kn}\delta_{lm}\Lambda_{ijk}\Lambda_{lmn} \\ &+\frac{1}{2}a_{4}\delta_{jk}\delta_{il}\delta_{mn}\Lambda_{ijk}\Lambda_{lmn} + \frac{1}{2}a_{5}\delta_{jk}\delta_{im}\delta_{nl}\Lambda_{ijk}\Lambda_{lmn} + \frac{1}{2}a_{1}\delta_{jk}\delta_{in}\delta_{lm}\Lambda_{ijk}\Lambda_{lmn} \\ &+\frac{1}{2}a_{5}\delta_{ki}\delta_{jl}\delta_{mn}\Lambda_{ijk}\Lambda_{lmn} + \frac{1}{2}a_{8}\delta_{ki}\delta_{jm}\delta_{nl}\Lambda_{ijk}\Lambda_{lmn} + \frac{1}{2}a_{2}\delta_{ki}\delta_{jn}\delta_{lm}\Lambda_{ijk}\Lambda_{lmn} \\ &+\frac{1}{2}a_{10}\delta_{il}\delta_{jm}\delta_{kn}\Lambda_{ijk}\Lambda_{lmn} + \frac{1}{2}a_{11}\delta_{jl}\delta_{km}\delta_{in}\Lambda_{ijk}\Lambda_{lmn} + \frac{1}{2}a_{11}\delta_{kl}\delta_{im}\delta_{jn}\Lambda_{ijk}\Lambda_{lmn} \\ &+\frac{1}{2}a_{13}\delta_{il}\delta_{jn}\delta_{km}\Lambda_{ijk}\Lambda_{lmn} + \frac{1}{2}a_{14}\delta_{jl}\delta_{kn}\delta_{im}\Lambda_{ijk}\Lambda_{lmn} + \frac{1}{2}a_{15}\delta_{kl}\delta_{in}\delta_{jm}\Lambda_{ijk}\Lambda_{lmn} \\ &+g_{1}\delta_{ij}\delta_{kl}\Upsilon_{ij}G_{kl} + g_{2}\delta_{ik}\delta_{jl}\Upsilon_{ij}G_{kl} + g_{2}\delta_{il}\delta_{jk}\Upsilon_{ij}G_{kl} \end{split}$$

or, expanding the Kronecker symbols, it yields a geometrical non-linear generalization of eq. (5.5) in Mindlin [1],

$$U = \frac{1}{2}\lambda G_{ii}G_{jj} + \mu G_{ij}G_{ij} + \frac{1}{2}b_{1}\Upsilon_{ii}\Upsilon_{jj} + \frac{1}{2}b_{2}\Upsilon_{ij}\Upsilon_{ij}$$

$$+ \frac{1}{2}b_{3}\Upsilon_{ij}\Upsilon_{ji} + g_{1}\Upsilon_{ii}G_{jj} + g_{2}(\Upsilon_{ij} + \Upsilon_{ji})G_{ij}$$

$$+ a_{1}\Lambda_{iik}\Lambda_{kmm} + a_{2}\Lambda_{iik}\Lambda_{jkj} + \frac{1}{2}a_{3}\Lambda_{iik}\Lambda_{jjk} + \frac{1}{2}a_{4}\Lambda_{ijj}\Lambda_{ikk}$$

$$+ a_{5}\Lambda_{ijj}\Lambda_{kik} + \frac{1}{2}a_{8}\Lambda_{iji}\Lambda_{kjk} + \frac{1}{2}a_{10}\Lambda_{ijk}\Lambda_{ijk} + a_{11}\Lambda_{ijk}\Lambda_{jki}$$

$$+ \frac{1}{2}a_{13}\Lambda_{ijk}\Lambda_{ikj} + \frac{1}{2}a_{14}\Lambda_{ijk}\Lambda_{jik} + \frac{1}{2}a_{15}\Lambda_{ijk}\Lambda_{kji}.$$
(65)

The aim of this Subsection is to identify the corresponding 18 isotropic micromorphic constitutive coefficients, i.e., λ , μ , b_1 , b_2 , b_3 , g_1 , g_2 , a_1 , a_2 , a_3 , a_4 , a_5 , a_8 , a_{10} , a_{11} , a_{13} , a_{14} and a_{15} . To do this, we impose the isotropic condition by assuming no dependence of the 5 elastic stiffness k_{η} , k_{τ} , $k_{d\eta}$, $k_{d\tau}$ and k_{ud} with respect to the orientation \hat{c} (or, in the present 3D case, to the co-latitude θ and to the longitude φ), i.e.,

$$k_{\eta}\left(\theta,\varphi\right) = \frac{\bar{k}_{\eta}}{4\pi}, \quad k_{\tau}\left(\theta,\varphi\right) = \frac{\bar{k}_{\tau}}{4\pi}, \quad k_{d\eta}\left(\theta,\varphi\right) = \frac{\bar{k}_{d\eta}}{4\pi}, \quad k_{d\tau}\left(\theta,\varphi\right) = \frac{\bar{k}_{d\tau}}{4\pi}, \tag{66}$$

$$k_{ud}(\theta,\varphi) = \frac{k_{ud}}{4\pi}, \quad \hat{c}_1 = \cos\theta\cos\varphi \quad \hat{c}_2 = \cos\theta\sin\varphi \quad \hat{c}_3 = \sin\theta,$$
 (67)

where \bar{k}_{η} , \bar{k}_{τ} , $\bar{k}_{d\eta}$, $\bar{k}_{d\tau}$ and \bar{k}_{ud} are the averaged stiffness over the unit sphere S^2 , that are defined in the general anisotropic case as follows,

$$\begin{split} \bar{k}_{\eta} &= \int_{0}^{2\pi} \left[\int_{0}^{\pi} k_{\eta} \left(\theta, \varphi \right) \sin \theta d\theta \right] d\varphi, \qquad \bar{k}_{\tau} = \int_{0}^{2\pi} \left[\int_{0}^{\pi} k_{\tau} \left(\theta, \varphi \right) \sin \theta d\theta \right] d\varphi, \\ \bar{k}_{d\eta} &= \int_{0}^{2\pi} \left[\int_{0}^{\pi} k_{d\eta} \left(\theta, \varphi \right) \sin \theta d\theta \right] d\varphi, \qquad \bar{k}_{d\tau} = \int_{0}^{2\pi} \left[\int_{0}^{\pi} k_{d\tau} \left(\theta, \varphi \right) \sin \theta d\theta \right] d\varphi, \\ \bar{k}_{ud} &= \int_{0}^{2\pi} \left[\int_{0}^{\pi} k_{ud} \left(\theta, \varphi \right) \sin \theta d\theta \right] d\varphi. \end{split}$$

Insertion of (66-67) into (48), (61), (62) and (63) yield the following and desired identification:

$$\lambda = \mathbb{C}_{1122} = \frac{L^2}{15} \left(\bar{k}_{\eta} - 4\bar{k}_{\tau} \right), \quad \mu = \mathbb{C}_{1212} = \frac{L^2}{15} \left(\bar{k}_{\eta} + 6\bar{k}_{\tau} \right)$$
 (68)

$$b_1 = \mathbb{B}_{1122} = \mathbb{B}_{1221} = b_3 = \frac{L^2}{15} \left(\bar{k}_{d\eta} - \bar{k}_{d\tau} \right), \quad \mathbb{B}_{1212} = b_2 = \frac{L^2}{15} \left(\bar{k}_{d\eta} + 4\bar{k}_{d\tau} \right), \tag{69}$$

$$\mathbb{G}_{1122} = g_1 = \mathbb{G}_{1212} = g_2 = \frac{L^2}{15} \bar{k}_{ud},\tag{70}$$

$$\mathbb{A}_{112233} = a_1 = \mathbb{A}_{112323} = a_2 = \mathbb{A}_{112332} = a_3 = \frac{L^4}{105} \left(\bar{k}_{d\eta} - \bar{k}_{d\tau} \right), \tag{71}$$

$$\mathbb{A}_{122133} = a_4 = \mathbb{A}_{122313} = a_5 = \mathbb{A}_{121323} = a_8 = \frac{L^4}{105} \left(\bar{k}_{d\eta} - \bar{k}_{d\tau} \right), \tag{72}$$

$$\mathbb{A}_{123231} = a_{11} = \mathbb{A}_{123132} = a_{13} = \mathbb{A}_{123213} = a_{14} = \frac{L^4}{105} \left(\bar{k}_{d\eta} - \bar{k}_{d\tau} \right) \tag{73}$$

$$\mathbb{A}_{123123} = a_{10} = \mathbb{A}_{123321} = a_{15} = \frac{L^4}{105} \left(\bar{k}_{d\eta} + 6\bar{k}_{d\tau} \right). \tag{74}$$

3.4 Linear 3D isotropic case for general micro deformation m^{np}

From the definition of the deformation gradient $F = \nabla \chi$ in $(9)_1$ and of the micromorphic deformation gradient P in (8), we define the displacement gradient H and the transpose micromorphic displacement gradient Ψ ,

$$\mathcal{F} = I + H, \quad \mathcal{P} = I + \Psi^T. \tag{75}$$

Thus, the first non-linear micro-deformation gradient, for small displacement approximations, is simplified from (13),

$$\Lambda_{ijh} = \mathcal{F}_{ha}^{-1} P_{aj,i} \cong (\delta_{ha} - H_{ha}) P_{aj,i} \cong \delta_{ha} P_{aj,i} = P_{hj,i} = \Psi_{jh,i} = \kappa_{ijh}, \tag{76}$$

and the second non-linear micro-deformation gradient, for small displacement approximations, is simplified from (14),

$$\Lambda_{ijh}^r = \mathcal{P}_{ah} P_{aj,i} = (\delta_{ah} + \Psi_{ha}) P_{aj,i} \cong \delta_{ah} P_{aj,i} = P_{hj,i} = \Psi_{jh,i} = \kappa_{ijh}, \tag{77}$$

that means that, in the linear approximation, the first Λ and the second Λ^r non-linear microdeformation gradients are the same third-order tensor κ , that is called the micro-deformation gradient. Besides, the Green-Saint-Venant tensor G (or non-linear macro-strain), the micromorphic Green-Saint-Venant tensor M and the micro-macro Green-Saint-Venant tensors Υ (or non-linear relative deformation), for small displacement approximations, are simplified from (10) and (11)

$$G = \frac{1}{2} (H + H^T + H^T H) \cong \frac{1}{2} (H + H^T) = \epsilon,$$
 (78)

$$\Upsilon \cong I - (I + \Psi) (I - H^T) \cong H^T - \Psi = \gamma, \tag{79}$$

$$M = \frac{1}{2} \left(\Psi + \Psi^T + \Psi \Psi^T \right) \cong \frac{1}{2} \left(\Psi + \Psi^T \right) = \frac{1}{2} \left(H^T - \gamma + H - \gamma^T \right) = \epsilon - \frac{1}{2} \left(\gamma + \gamma^T \right), \tag{80}$$

that means from (80) that, in the linear approximation, the micromorphic Green-Saint-Venant tensor M depends upon the Green-Saint-Venant tensor G and upon the micro-macro Green-Saint-Venant tensor Υ and it is not anymore an independent strain measure. Besides, the non-linear macro-strain G is simplified from (78) in the macro strain ϵ and the non-linear relative deformation Υ is simplified from (79) in the relative deformation γ . Thus, the three strain measure from (78), (79) and (76) are the same defined in Mindlin [1] respectively in eqns. (1.10), (1.11) and (1.12), viz.,

$$\epsilon_{ij} = \frac{1}{2} (u_{i,j} + u_{j,i}), \quad \gamma_{ij} = u_{j,i} - \Psi_{ij}, \quad \kappa_{ijk} = \Psi_{jk,i}$$
(81)

Insertion of the linear approximations (76-80) into the general form of the elastic energy (47), yields

$$U = \frac{1}{2} \mathbb{C}_{ijkl}^n \epsilon_{ij} \epsilon_{kl} + \frac{1}{2} \mathbb{B}_{ijkl}^n \gamma_{ij} \gamma_{kl} + \frac{1}{2} \mathbb{A}_{ijhabc}^n \kappa_{ijh} \kappa_{abc}$$
 (82)

$$+\mathbb{D}_{ijklm}^{n}\gamma_{ij}\kappa_{klm} + \mathbb{F}_{ijklm}^{n}\kappa_{ijk}\epsilon_{lm} + \mathbb{G}_{ijkl}^{n}\gamma_{ij}\epsilon_{kl}$$
(83)

where new constitutive tensors (with the super-script n) are defined in terms of that defined in (48-58),

$$\mathbb{C}_{ijkl}^n = \mathbb{C}_{ijkl} + \mathbb{C}_{ijkl}^r + 2\mathbb{G}_{ijkl}^r, \tag{84}$$

$$\mathbb{B}_{ijkl}^n = \mathbb{B}_{ijkl} + \mathbb{C}_{(ij)(kl)}^r + 2\mathbb{B}_{(ij)kl}^r, \tag{85}$$

$$\mathbb{A}_{ijhabc}^{n} = \mathbb{A}_{ijhabc} + \mathbb{A}_{ijhabc}^{r}, \tag{86}$$

$$\mathbb{D}_{ijklm}^{n} = \mathbb{D}_{ijklm} + \mathbb{D}_{(ij)klm}^{r} + \mathbb{D}_{[ij]klm}^{rr}, \tag{87}$$

$$\mathbb{F}_{ijklm}^n = \mathbb{F}_{ijklm} + \mathbb{D}_{lmijk}^r - \mathbb{D}_{lmijk}^{rr} + \mathbb{F}_{ijklm}^r, \tag{88}$$

$$\mathbb{G}_{ijkl}^n = \mathbb{G}_{ijkl} + \mathbb{C}_{ij(kl)}^r + \mathbb{G}_{(ij)kl}^r + \mathbb{B}_{ijkl}^r, \tag{89}$$

where the symmetrization and skew-symmetrization rules

$$A_{(ij)} = \frac{1}{2} (A_{ij} + A_{ji}), \qquad A_{[ij]} = \frac{1}{2} (A_{ij} - A_{ji}),$$

have been used in (84-89). Insertion of (48-58) into (84-89) yields the explicit identification of the new constitutive tensors,

$$\mathbb{C}_{ijkl}^{n} = L^{2} \int_{\mathcal{S}^{2}} (k_{\eta} - 4k_{\tau} + 4k_{r\eta} - 4k_{r\tau} + 2k_{ur}) \,\hat{c}_{i} \hat{c}_{j} \hat{c}_{k} \hat{c}_{l} \tag{90}$$

$$+L^{2}\int_{\mathbb{S}^{2}}\left(k_{\tau}+k_{r\tau}\right)\left(\delta_{ik}\hat{c}_{j}\hat{c}_{l}+\delta_{il}\hat{c}_{j}\hat{c}_{k}+\delta_{jk}\hat{c}_{i}\hat{c}_{l}+\delta_{jl}\hat{c}_{i}\hat{c}_{k}\right),$$

$$\mathbb{B}_{ijkl}^{n} = L^{2} \int_{\mathcal{S}^{2}} \left[\left(k_{d\eta} - k_{d\tau} + 4k_{r\eta} - 4k_{r\tau} + 4k_{rd} \right) \hat{c}_{i} \hat{c}_{k} \hat{c}_{j} \hat{c}_{l} \right]$$
(91)

$$+L^{2}\int_{\mathcal{S}^{2}}\left(k_{r\tau}+k_{d\tau}\right)\left(\delta_{ik}\hat{c}_{j}\hat{c}_{l}\right)+k_{r\tau}\left(\delta_{il}\hat{c}_{j}\hat{c}_{k}+\delta_{jk}\hat{c}_{i}\hat{c}_{l}+\delta_{jl}\hat{c}_{i}\hat{c}_{k}\right),$$

$$\mathbb{A}_{ijhabc}^{n} = L^{4} \int_{\mathcal{S}^{2}} \left[\left(k_{d\eta} - k_{d\tau} + \frac{1}{2} k_{r\eta} - \frac{1}{2} k_{r\tau} - k_{rd} \right) \hat{c}_{j} \hat{c}_{b} + \left(k_{d\tau} + \frac{1}{2} k_{r\tau} \right) \delta_{jb} \right] \hat{c}_{i} \hat{c}_{h} \hat{c}_{a} \hat{c}_{c}, (92)$$

$$\mathbb{D}_{ijabc}^{n} = L^{3} \int_{S^{2}} \left[\left(-k_{d\eta} + k_{d\tau} + 2k_{r\eta} - 2k_{r\tau} \right) \hat{c}_{i} \hat{c}_{b} \hat{c}_{j} + \left(k_{r\tau} - k_{d\tau} \right) \delta_{ib} \hat{c}_{j} + k_{r\tau} \hat{c}_{i} \delta_{jb} \right] \hat{c}_{a} \hat{c}_{c}, \quad (93)$$

$$\mathbb{F}_{ijklm}^{n} = L^{3} \int_{\mathcal{S}^{2}} \left(k_{ur} - k_{ud} + 2k_{r\eta} - 2k_{r\tau} - k_{rd} \right) \hat{c}_{i} \hat{c}_{j} \hat{c}_{k} \hat{c}_{l} \hat{c}_{m} + k_{r\tau} \left[\left(\hat{c}_{j} \delta_{ib} + \hat{c}_{i} \delta_{jb} \right) \right] \hat{c}_{a} \hat{c}_{c}, \quad (94)$$

$$\mathbb{G}_{ijkl}^{n} = L^{2} \int_{\mathcal{S}^{2}} (k_{ud} + k_{ur} + 4k_{r\eta} - 4k_{r\tau} + 2k_{rd}) \, \hat{c}_{i} \hat{c}_{j} \hat{c}_{k} \hat{c}_{l}, \tag{95}$$

In the isotropic case, among (66) and (67), we assume also the independence of the remaining stiffness with respect to the unit vector \hat{c} , i.e.,

$$k_{r\eta}(\theta,\varphi) = \frac{\bar{k}_{r\eta}}{4\pi}, \qquad k_{r\tau}(\theta,\varphi) = \frac{\bar{k}_{r\tau}}{4\pi}, \qquad k_{ur}(\theta,\varphi) = \frac{\bar{k}_{ur}}{4\pi}, \qquad k_{rd}(\theta,\varphi) = \frac{\bar{k}_{rd}}{4\pi}.$$
 (96)

In this case the Lame's constant in (68) are differently identified from insertion of (66-67-96) into (90)

$$\lambda = \mathbb{C}_{1122}^n = \frac{1}{15} L^2 \left(\bar{k}_{\eta} - 4\bar{k}_{\tau} + 4\bar{k}_{r\eta} - 4\bar{k}_{r\tau} + 2\bar{k}_{ur} \right) \tag{97}$$

$$\mu = \mathbb{C}_{1212}^n = \frac{1}{15} L^2 \left(\bar{k}_{\eta} + 6\bar{k}_{\tau} + 4\bar{k}_{r\eta} + 6\bar{k}_{r\tau} + 2\bar{k}_{ur} \right) \tag{98}$$

so that the Young's modulus and the Poisson's ratio,

$$Y = \mu \frac{3\lambda + 2\mu}{\lambda + \mu}, \quad \nu = \frac{\lambda}{2(\lambda + \mu)}, \tag{99}$$

are identified as

$$Y = \frac{1}{15}L^2 \left(\bar{k}_{\eta} + 6\bar{k}_{\tau} + 4\bar{k}_{r\eta} + 6\bar{k}_{r\tau} + 2\bar{k}_{ur} \right) \frac{\left(5\bar{k}_{\eta} + 20\bar{k}_{r\eta} + 10\bar{k}_{ur} \right)}{2 \left(\bar{k}_{\eta} + \bar{k}_{\tau} + 4\bar{k}_{r\eta} + \bar{k}_{r\tau} + 2\bar{k}_{ur} \right)}, \tag{100}$$

$$\nu = \frac{\left(\bar{k}_{\eta} - 4\bar{k}_{\tau} + 4\bar{k}_{r\eta} - 4\bar{k}_{r\tau} + 2\bar{k}_{ur}\right)}{4\left(\bar{k}_{\eta} + \bar{k}_{\tau} + 4\bar{k}_{r\eta} + \bar{k}_{r\tau} + 2\bar{k}_{ur}\right)}$$
(101)

These expressions for the stiffness parameters in 90 to 95 provide an essential seed for an initial estimation of all the elastic parameters that characterize a micromorphic continuum. It is remarkable that these first estimates indicate that such materials are described by several characteristic lengths, which can be multiples of relevant grain-size, and represent the influence of grain-scale micro-mechanisms on the emergent behavior at the macro-scale. These micromechanisms may include those that resemble the floppy behavior of pantograph, best described by second-gradient macro-scale continua analyzed in [35,86], or other mechanisms that require additional kinematical

descriptors to capture the deformation energy of grain-pair [7,17,51,71]. It is also noteworthy that it is possible to estimate the elastic parameters a micromorphic continuum in terms of a few parameters that link to the micro-mechanisms without recourse to *ad hoc* prescriptions or *a priori* (over) simplifications. For certain, relatively simple micro-mechanisms and structures, such linkages can indeed be identified, synthesized and experimentally characterized as discussed in [51,52] and [42–50,87–90].

4 Conclusion

For accurate and tractable description of the mechanical behavior of a large class of materials which at some spatial scale possess granular microstructure, refined models, such as the micromorphic models, are needed. Such models are particularly significant for bridging, in a heuristic way, across spatial scales ranging from that at grain interactions to collective behavior of large numbers of grains. At meso-scales of few grains to tens of thousands of grains, discrete simulations can be conceived that provide the trajectories and distribution of grain-scale deformation energies. It is worthwhile to note here that although discrete models have proliferated over the past several decades, their systematic validation through experimentally measured particle trajectories and grain-scale energy distributions have been characteristically sparse (absent to the knowledge of these authors). At the macro-scales consisting of large number of grains of various sizes, interfaces/surfaces, composition and arrangement (collectively micro-mechano-morphology), discrete models could be intractable. In these cases, micromorphic continuum models can serve as effective reduced-order models that can capture many essential aspects of the grain-scale mechanisms. This paper describes an approach to construct such micromorphic models in the framework of finite (geometrically nonlinear) deformations using the concepts of granular micromechanics. The key aspect of the described approach is the identification of the appropriate kinematic measures that describe the macro-deformation and link it to the micro-deformation, formulation of the deformation energies in terms of these measures and the application of energy methods to identify the constitutive relations. Such an approach permits potential identification of inner deformation modes that store elastic energy contributing to the emergent behavior at the macro-scale, and indicates the pathway to access these modes with the view of rational design of (meta) materials.

Furthermore, we would like to identify a number of potential outlook of the presented approach. First, the isotropic identification we have shown can be extended to an anisotropic one by the use of proper non constant orientation distribution function instead of (66-67-96). Second, the truncation of the Taylor's series expansions (18-19) up to the first order in terms of the kinematic descriptors results in a first-grade continuum theory. Such a limitation can be removed to obtain higher order gradient continuum theories without unduly augmenting the number of the constitutive coefficients that need to be experimentally identified. Third, the quadratic assumption (46) can be generalized, such as with Leonard-Jones type potential to take into account elastic-hardening effects and tension-compression asymmetry that can lead to emergence of anisotropy. Fourth, dissipative phenomena such as damage [84] and plasticity [91] can be included by using for example an hemivariational approach or by assuming dissipation energy in terms of additional entropic irreversible kinematical descriptors. It is further remarkable that plastic deformation in the present micromorphic form can give rise to inelastic microstructural rotation.

Acknowledgement

AM is supported in part by the United States National Science Foundation grant CMMI -1727433.

References

- [1] R. D. Mindlin. Micro-structure in linear elasticity. Archive for Rational Mechanics and Analysis, 16(1):51–78, 1964.
- [2] P. Germain. The method of virtual power in continuum mechanics. Part 2: Microstructure. Siam Journal on Applied Mathematics, 25(3):556–575, 1973.

- [3] A Cemal Eringen. Microcontinuum field theories: foundations and solids, volume 487. Springer New York, 1999.
- [4] Victor A. Eremeyev. On the material symmetry group for micromorphic media with applications to granular materials. *Mechanics Research Communications*, 94:8–12, 2018.
- [5] H. Hertz. On the contact of elastic solids. Journal fur de reine und angewandte Mathematik, 92:156-171, 1881.
- [6] R. D. Mindlin and H. Deresiewicz. Elastic spheres in contact under varying oblique forces. Journal of Applied Mechanics-Transactions of the Asme, 20(3):327-344, 1953.
- [7] P. Poorsolhjouy and A. Misra. Granular micromechanics based continuum model for grain rotations and grain rotation waves. *Journal of the Mechanics and Physics of Solids*, 129:244– 260, 2019.
- [8] Elena A Ivanova. On the use of the continuum mechanics method for describing interactions in discrete systems with rotational degrees of freedom. *Journal of Elasticity*, 133(2):155–199, 2018.
- [9] A.-L. Cauchy. Sur l'equilibre et le mouvement d'un systeme de points materiels sollicites par des forces d'attraction ou de repulsion mutuelle. Excercises de Mathematiques, 3:188-212, 1826-1830.
- [10] C.L. Navier. Sur les lois de l'equilibre et du mouvement des corps solides elastiques. *Memoire de l'Academie Royale de Sciences*, 7:375–393, 1827.
- [11] Francesco dell'Isola, Giulio Maier, Umberto Perego, Ugo Andreaus, Raffaele Esposito, and Samuel Forest. The complete works of Gabrio Piola: Volume I Commented English Translation English and Italian Edition. Springer Publishing Company, Incorporated, 2014.
- [12] Herman Berendsen. Simulating the physical world. Cambridge University Press Cambridge, 2007.
- [13] K Eric Drexler. Nanosystems: molecular machinery, manufacturing, and computation. New York: John Wiley & Sons, 1992.
- [14] Emilio Turco, Francesco dell'Isola, and Anil Misra. A nonlinear lagrangian particle model for grains assemblies including grain relative rotations. *International Journal for Numerical and Analytical Methods in Geomechanics*, 43(5):1051–1079, 2019.
- [15] R Holtzman, Dmitriy B Silin, and Tad W Patzek. Frictional granular mechanics: A variational approach. *International journal for numerical methods in engineering*, 81(10):1259–1280, 2010.
- [16] A Misra, L Placidi, and E Turco. Variational methods for continuum models of granular materials. Encyclopedia of Continuum Mechanics, Springer Berlin Heidelberg, Berlin, Heidelberg, pages 1–11, 2019.
- [17] Nima Nejadsadeghi and Anil Misra. Extended granular micromechanics approach: a micromorphic theory of degree n. *Mathematics and Mechanics of Solids*, 25(2):407–429, 2020.
- [18] Anil Misra and Payam Poorsolhjouy. Grain-and macro-scale kinematics for granular micromechanics based small deformation micromorphic continuum model. *Mechanics Research Com*munications, 81:1–6, 2017.
- [19] Emilio Turco, Anil Misra, Marek Pawlikowski, Francesco dell'Isola, and François Hild. Enhanced Piola-Hencky discrete models for pantographic sheets with pivots without deformation energy: numerics and experiments. *International Journal of Solids and Structures*, 147:94–109, 2018.
- [20] Emilio Turco, Anil Misra, Rizacan Sarikaya, and Tomasz Lekszycki. Quantitative analysis of deformation mechanisms in pantographic substructures: experiments and modeling. *Continuum Mechanics and Thermodynamics*, 31(1):209–223, 2019.

- [21] Emilio Turco and Emilio Barchiesi. Equilibrium paths of Hencky pantographic beams in a three-point bending problem. *Mathematics and Mechanics of Complex Systems*, 7(4):287–310, 2019.
- [22] Emilio Turco, Emilio Barchiesi, Ivan Giorgio, and Francesco dell'Isola. A Lagrangian Henckytype non-linear model suitable for metamaterials design of shearable and extensible slender deformable bodies alternative to Timoshenko theory. *International Journal of Non-Linear Mechanics*, 123, 2020.
- [23] F. dell'Isola, E. Turco, and E. Barchiesi. 5. Lagrangian discrete models: Applications to metamaterials. Discrete and Continuum Models for Complex Metamaterials, page 197, 2020.
- [24] Boris Desmorat, Mario Spagnuolo, and Emilio Turco. Stiffness optimization in nonlinear pantographic structures. *Mathematics and Mechanics of Solids*, 25(12):2252–2262, 2020.
- [25] Emilio Turco. Modelling of two-dimensional Timoshenko beams in Hencky fashion. In Developments and Novel Approaches in Nonlinear Solid Body Mechanics, pages 159–177. Springer, 2020.
- [26] Emilio Turco. Stepwise analysis of pantographic beams subjected to impulsive loads. *Mathematics and Mechanics of Solids*, 2020.
- [27] Victor A Eremeyev and Emilio Turco. Enriched buckling for beam-lattice metamaterials. *Mechanics Research Communications*, 103, 2020.
- [28] Alessandro Della Corte, Antonio Battista, Francesco dell'Isola, and Ivan Giorgio. Modeling deformable bodies using discrete systems with centroid-based propagating interaction: fracture and crack evolution. In *Mathematical Modelling in Solid Mechanics*, pages 59–88. Springer, 2017.
- [29] E. Turco, F. dell'Isola, N.L. Rizzi, R. Grygoruk, W.H. Müller, and C. Liebold. Fiber rupture in sheared planar pantographic sheets: Numerical and experimental evidence. *Mechanics Research Communications*, 76:86–90, 2016.
- [30] Anil Misra, L Ouyang, Jie Chen, and WY Ching. Ab initio calculations of strain fields and failure patterns in silicon nitride intergranular glassy films. *Philosophical Magazine*, 87(25):3839– 3852, 2007.
- [31] Jun Chen, Lizhi Ouyang, Paul Rulis, Anil Misra, and Wai-Yim Ching. Complex nonlinear deformation of nanometer intergranular glassy films in β si 3 n 4. *Physical review letters*, 95(25):256103, 2005.
- [32] John F Peters and Laura E Walizer. Patterned nonaffine motion in granular media. *Journal of Engineering Mechanics*, 139(10):1479–1490, 2013.
- [33] Antoinette Tordesillas, Sebastian Pucilowski, Qun Lin, John F Peters, and Robert P Behringer. Granular vortices: identification, characterization and conditions for the localization of deformation. Journal of the Mechanics and Physics of Solids, 90:215-241, 2016.
- [34] A. Misra and W. Y. Ching. Theoretical nonlinear response of complex single crystal under multi-axial tensile loading. *Sci Rep*, 3:1488, 2013.
- [35] J-J. Alibert, P. Seppecher, and F. dell'Isola. Truss modular beams with deformation energy depending on higher displacement gradients. *Mathematics and Mechanics of Solids*, 8(1):51–73, 2003.
- [36] Trushant S. Majmudar and Robert P. Behringer. Contact force measurements and stress-induced anisotropy in granular materials. *Nature*, 435(7045):1079, 2005.
- [37] Antoinette Tordesillas, Jie Zhang, and Robert Behringer. Buckling force chains in dense granular assemblies: physical and numerical experiments. Geomechanics and Geoengineering: An International Journal, 4(1):3–16, 2009.

- [38] Lingran Zhang, Nho Gia Hien Nguyen, Stephane Lambert, Francois Nicot, Florent Prunier, and Irini Djeran-Maigre. The role of force chains in granular materials: from statics to dynamics. European Journal of Environmental and Civil Engineering, 21(7-8):874–895, 2017.
- [39] A. Misra and H. Jiang. Measured kinematic fields in the biaxial shear of granular materials. Computers and Geotechnics, 20(3-4):267–285, 1997.
- [40] V. Richefeu, G. Combe, and G. Viggiani. An experimental assessment of displacement fluctuations in a 2D granular material subjected to shear. *Geotechnique Letters*, 2:113–118, 2012.
- [41] Francesco dell'Isola, Emilio Barchiesi, and Anil Misra. Naive Model Theory: its applications to the Theory of Metamaterials Design, pages 141–196. Cambridge, 2020.
- [42] F. dell'Isola, I. Giorgio, M. Pawlikowski, and N. Rizzi. Large deformations of planar extensible beams and pantographic lattices: heuristic homogenization, experimental and numerical examples of equilibrium. *Proc. R. Soc. A*, 472(2185), 2016.
- [43] Francesco dell'Isola, Pierre Seppecher, Jean Jacques Alibert, Tomasz Lekszycki, Roman Grygoruk, Marek Pawlikowski, David Steigmann, Ivan Giorgio, Ugo Andreaus, Emilio Turco, Maciej Golaszewski, Nicola Rizzi, Claude Boutin, Victor A. Eremeyev, Anil Misra, Luca Placidi, Emilio Barchiesi, Leopoldo Greco, Massimo Cuomo, Antonio Cazzani, Alessandro Della Corte, Antonio Battista, Daria Scerrato, Inna Zurba Eremeeva, Yosra Rahali, Jean-Francois Ganghoffer, Wolfgang Mueller, Gregor Ganzosch, Mario Spagnuolo, Aron Pfaff, Katarzyna Barcz, Klaus Hoschke, Jan Neggers, and Francois Hild. Pantographic metamaterials: an example of mathematically driven design and of its technological challenges. Continuum Mechanics and Thermodynamics, 31(4):851–884, 2018.
- [44] Francesco dell'Isola, Pierre Seppecher, Mario Spagnuolo, Emilio Barchiesi, François Hild, Tomasz Lekszycki, Ivan Giorgio, Luca Placidi, Ugo Andreaus, Massimo Cuomo, et al. Advances in pantographic structures: design, manufacturing, models, experiments and image analyses. Continuum Mechanics and Thermodynamics, 31(4):1231–1282, 2019.
- [45] I Giorgio, NL Rizzi, and E Turco. Continuum modelling of pantographic sheets for out-ofplane bifurcation and vibrational analysis. *Proceedings of the Royal Society A: Mathematical*, *Physical and Engineering Sciences*, 473(2207), 2017.
- [46] C. Boutin, I. Giorgio, L. Placidi, et al. Linear pantographic sheets: Asymptotic micro-macro models identification. *Mathematics and Mechanics of Complex Systems*, 5(2):127–162, 2017.
- [47] Emilio Barchiesi, Francesco dell'Isola, and François Hild. On the validation of homogenized modeling for bi-pantographic metamaterials via digital image correlation. *International Journal of Solids and Structures*, 208:49–62, 2021.
- [48] Luca Placidi, Francesco dell'Isola, and Emilio Barchiesi. Heuristic homogenization of Euler and pantographic beams. In *Mechanics of Fibrous Materials and Applications*, pages 123–155. Springer, 2020.
- [49] Emilio Barchiesi, Simon R Eugster, Francesco Dell'isola, and François Hild. Large in-plane elastic deformations of bi-pantographic fabrics: asymptotic homogenization and experimental validation. *Mathematics and Mechanics of Solids*, 25(3):739–767, 2020.
- [50] Y. Rahali, I. Giorgio, J.F. Ganghoffer, and F. dell'Isola. Homogenization à la Piola produces second gradient continuum models for linear pantographic lattices. *International Journal of Engineering Science*, 97:148–172, 2015.
- [51] Ivan Giorgio, Francesco dell'Isola, and Anil Misra. Chirality in 2D cosserat media related to stretch-micro-rotation coupling with links to granular micromechanics. *International Journal of Solids and Structures*, 202:28–38, 2020.
- [52] Anil Misra, Nima Nejadsadeghi, Michele De Angelo, and Luca Placidi. Chiral metamaterial predicted by granular micromechanics: verified with 1D example synthesized using additive manufacturing. *Continuum Mechanics and Thermodynamics*, pages 1–17, 2020.

- [53] Emilio Barchiesi and Sergei Khakalo. Variational asymptotic homogenization of beam-like square lattice structures. *Mathematics and Mechanics of Solids*, 24(10):3295–3318, 2019.
- [54] Mohamed Camar-Eddine and Pierre Seppecher. Non-local interactions resulting from the homogenization of a linear diffusive medium. Comptes Rendus de l'Académie des Sciences-Series I-Mathematics, 332(5):485–490, 2001.
- [55] James Utama Surjadi, Libo Gao, Huifeng Du, Xiang Li, Xiang Xiong, Nicholas Xuanlai Fang, and Yang Lu. Mechanical metamaterials and their engineering applications. Advanced Engineering Materials, 21(3), 2019.
- [56] Ivan Giorgio, Mario Spagnuolo, Ugo Andreaus, Daria Scerrato, and Alberto Maria Bersani. Indepth gaze at the astonishing mechanical behavior of bone: A review for designing bio-inspired hierarchical metamaterials. *Mathematics and Mechanics of Solids*, page 1081286520978516, 2020.
- [57] Mario Spagnuolo, M Erden Yildizdag, Ugo Andreaus, and Antonio M Cazzani. Are higher-gradient models also capable of predicting mechanical behavior in the case of wide-knit pantographic structures? *Mathematics and Mechanics of Solids*, 26(1):18–29, 2021.
- [58] M Spagnuolo, P Franciosi, and F dell'Isola. A Green operator-based elastic modeling for two-phase pantographic-inspired bi-continuous materials. *International Journal of Solids and Structures*, 188:282–308, 2020.
- [59] F dell'Isola, P Seppecher, L Placidi, E Barchiesi, and A Misra. 8: Least action and virtual work principles for the formulation of generalized continuum models. *Discrete and Continuum Models for Complex Metamaterials*, page 327, 2020.
- [60] Luca Placidi, Giuseppe Rosi, and Emilio Barchiesi. Analytical solutions of 2-dimensional second gradient linear elasticity for continua with cubic-D4 microstructure. In New Achievements in Continuum Mechanics and Thermodynamics, pages 383-401. Springer, 2019.
- [61] Emilio Barchiesi, Hua Yang, Chuong Anthony Tran, Luca Placidi, and Wolfgang H Müller. Computation of brittle fracture propagation in strain gradient materials by the FEniCS library. *Mathematics and Mechanics of Solids*, 2020.
- [62] Chuong Anthony Tran, Maciej Gołaszewski, and Emilio Barchiesi. Symmetric-in-plane compression of polyamide pantographic fabrics modelling, experiments and numerical exploration. Symmetry, 12(5):693, 2020.
- [63] M Erden Yildizdag, Emilio Barchiesi, and Francesco dell'Isola. Three-point bending test of pantographic blocks: numerical and experimental investigation. *Mathematics and Mechanics of Solids*, 25(10):1965–1978, 2020.
- [64] Yury Solyaev, Sergey Lurie, Emilio Barchiesi, and Luca Placidi. On the dependence of standard and gradient elastic material constants on a field of defects. *Mathematics and Mechanics of Solids*, 25(1):35–45, 2020.
- [65] Luca Placidi, Anil Misra, and Emilio Barchiesi. Simulation results for damage with evolving microstructure and growing strain gradient moduli. *Continuum Mechanics and Thermodynamics*, 31(4):1143–1163, 2019.
- [66] Emilio Turco, Ivan Giorgio, Anil Misra, and Francesco dell'Isola. King post truss as a motif for internal structure of (meta) material with controlled elastic properties. *Royal Society open science*, 4(10), 2017.
- [67] Luca Placidi, Anil Misra, and Emilio Barchiesi. Two-dimensional strain gradient damage modeling: a variational approach. Zeitschrift für angewandte Mathematik und Physik, 69(3):56, 2018.
- [68] Luca Placidi, Emilio Barchiesi, and Anil Misra. A strain gradient variational approach to damage: a comparison with damage gradient models and numerical results. *Mathematics and Mechanics of Complex Systems*, 6(2):77–100, 2018.

- [69] Anil Misra, Tomasz Lekszycki, Ivan Giorgio, Gregor Ganzosch, Wolfgang H Müller, and Francesco Dell'Isola. Pantographic metamaterials show atypical poynting effect reversal. Mechanics Research Communications, 89:6–10, 2018.
- [70] Emilio Barchiesi, Francesco dell'Isola, Alberto M Bersani, and Emilio Turco. Equilibria determination of elastic articulated duoskelion beams in 2D via a Riks-type algorithm. *International Journal of Non-Linear Mechanics*, 128.
- [71] Michele De Angelo, Luca Placidi, Nima Nejadsadeghi, and Anil Misra. Non-standard Timoshenko beam model for chiral metamaterial: identification of stiffness parameters. *Mechanics Research Communications*, 2019.
- [72] Ivan Giorgio, Michele De Angelo, Emilio Turco, and Anil Misra. A Biot-Cosserat two-dimensional elastic nonlinear model for a micromorphic medium. *Continuum Mechanics and Thermodynamics*, pages 1–13, 2019.
- [73] Leonid P. Lebedev, Michael J. Cloud, and Victor A. Eremeyev. *Tensor analysis with applications in mechanics*. World Scientific, 2010.
- [74] H. Altenbach and V. Eremeyev. On the linear theory of micropolar plates. ZAMM-Journal of Applied Mathematics and Mechanics/Zeitschrift für Angewandte Mathematik und Mechanik, 89(4):242–256, 2009.
- [75] W. Pietraszkiewicz and V. Eremeyev. On natural strain measures of the non-linear micropolar continuum. *International Journal of Solids and Structures*, 46(3):774–787, 2009.
- [76] Victor A Eremeyev, Leonid P Lebedev, and Holm Altenbach. Foundations of micropolar mechanics. Springer Science & Business Media, 2012.
- [77] Johannes Altenbach, Holm Altenbach, and Victor A. Eremeyev. On generalized Cosserat-type theories of plates and shells: a short review and bibliography. *Archive of Applied Mechanics*, 80(1):73–92, 2010.
- [78] Victor A Eremeyev. On the characterization of the nonlinear reduced micromorphic continuum with the local material symmetry group. In *Higher gradient materials and related generalized continua*, pages 43–54. Springer, 2019.
- [79] Anil Misra and Payam Poorsolhjouy. Elastic behavior of 2D grain packing modeled as micro-morphic media based on granular micromechanics. *Journal of Engineering Mechanics*, 143(1), 2017.
- [80] Arkadi Berezovski, Ivan Giorgio, and Alessandro Della Corte. Interfaces in micromorphic materials: wave transmission and reflection with numerical simulations. *Mathematics and Mechanics of Solids*, 21(1):37–51, 2016.
- [81] Anil Misra and Payam Poorsolhjouy. Granular micromechanics based micromorphic model predicts frequency band gaps. *Continuum Mechanics and Thermodynamics*, 28(1-2):215–234, 2016.
- [82] Milad Shirani, Cheng Luo, and David J Steigmann. Cosserat elasticity of lattice shells with kinematically independent flexure and twist. *Continuum Mechanics and Thermodynamics*, 31(4):1087–1097, 2019.
- [83] Milad Shirani and David J Steigmann. A cosserat model of elastic solids reinforced by a family of curved and twisted fibers. *Symmetry*, 12(7):1133, 2020.
- [84] Dmitry Timofeev, Emilio Barchiesi, Anil Misra, and Luca Placidi. Hemivariational continuum approach for granular solids with damage-induced anisotropy evolution. *Mathematics and Mechanics of Solids*, 2020.
- [85] Haipeng Jia, Anil Misra, Payam Poorsolhjouy, and Congyi Liu. Optimal structural topology of materials with micro-scale tension-compression asymmetry simulated using granular micromechanics. *Materials & Design*, 115:422–432, 2017.

- [86] P. Seppecher, J.-J. Alibert, and F. dell'Isola. Linear elastic trusses leading to continua with exotic mechanical interactions. In *Journal of Physics: Conference Series*, volume 319. IOP Publishing, 2011.
- [87] Ivan Giorgio. A discrete formulation of kirchhoff rods in large-motion dynamics. *Mathematics and Mechanics of Solids*, 25(5):1081–1100, 2020.
- [88] Ivan Giorgio. Lattice shells composed of two families of curved kirchhoff rods: an archetypal example, topology optimization of a cycloidal metamaterial. *Continuum Mechanics and Thermodynamics*, pages 1–20, 2020.
- [89] Ivan Giorgio, Alessandro Ciallella, and Daria Scerrato. A study about the impact of the topological arrangement of fibers on fiber-reinforced composites: some guidelines aiming at the development of new ultra-stiff and ultra-soft metamaterials. *International Journal of Solids and Structures*, 203:73–83, 2020.
- [90] Hua Yang, Gregor Ganzosch, Ivan Giorgio, and B Emek Abali. Material characterization and computations of a polymeric metamaterial with a pantographic substructure. Zeitschrift für angewandte Mathematik und Physik, 69(4):1–16, 2018.
- [91] Luca Placidi, Emilio Barchiesi, Anil Misra, and Dmitry Timofeev. Micromechanics-based elastoplastic-damage energy formulation for strain gradient solids with granular microstructure. *Con*tinuum Mechanics and Thermodynamics, pages 1–29, 2021.